Title: Mutations and predicted glycosylation patterns in respiratory syncytial virus isolates correlate with disease severity.

Authors: Hunte Morgan L[1,2], Herbst Katherine W [3], Michelow Ian C[** 3,4,5], Szczepanek Steven M[* 1,2]

1. Department of Pathobiology, University of Connecticut, Storrs, CT, USA
2. Center of Excellence for Vaccine Research, University of Connecticut, Storrs, CT, USA
3. Connecticut Children's Research Institute, Connecticut Children's, Hartford, CT, USA
4. Division of Infectious Disease and Immunology, Connecticut Children's, Hartford, CT, USA
5. Department of Pediatrics, University of Connecticut School of Medicine, Farmington, CT, USA

***Corresponding author:**

Steven M. Szczepanek, Ph.D.
University of Connecticut
61 North Eagleville Road (Atwater Laboratory)
Storrs, CT 06238
Ph: 860-486-8101
Steven.Szczepanek@uconn.edu

****Co-Corresponding author:**

Ian C. Michelow, M.D
Connecticut Children's
85 Seymour Street, Suite 816
Hartford, CT 06106
Ph: 860-545-9490
Fax: 860-545-9371
IMichelow@connecticutchildrens.org

Abstract

Respiratory syncytial virus (RSV) remains an important cause of lower respiratory tract infections in young children, producing mild to life-threatening disease. Although rapid viral evolution through genetic drift is well established, the structural and functional impacts of specific pathoadaptive mutations linked to enhanced virulence are poorly defined. We investigated these relationships by isolating RSV from available nasal swabs of five hospitalized infants during the 2022–2023 winter season and conducting comparative viral genomic analysis. Severity of disease was evaluated using a validated clinical scoring system. Whole-genome sequencing followed by reference-guided assembly and structural modeling revealed distinct amino acid polymorphisms correlating with disease severity. Phylogenetic analysis placed all isolates within the RSV-A GA2.3.5 G clade. Isolates from mild moderate and severe cases clustered in A.D.1.5 and A.D.1.8 subclades. Nineteen amino acid differences were associated with clinical severity and isolates from moderate or severe cases replicated more rapidly in vitro than mild isolates. Computational glycosylation predictions indicated an increasing number of glycosylation sites in the G protein corresponding with greater disease severity. Together, these data suggest that specific pathoadaptive mutations may contribute to enhanced viral replication and severity, and are relevant for future surveillance efforts and the development of immune-based strategies targeting virulence-associated residues.

Key Words: Respiratory syncytial virus, genetic mutations, clinical severity, attachment glycoprotein, RNA polymerase

Introduction

Respiratory syncytial virus (RSV) remains a leading global cause of lower respiratory tract infections in infants and young children (1–3). Virtually all children acquire RSV infection at least once by 2 years of age (4). Although premature neonates, immunocompromised individuals and those with congenital heart, chronic lung or neuromuscular disorders are at great risk for severe disease, most severe cases occur in previously healthy, full-term infants. Factors contributing to severe disease in healthy children remain unknown (5,6).

The intrinsic mutability of RSV, owing to its RNA-dependent RNA polymerase, allows it to explore a vast sequence space, generating variants with potential fitness advantages (7,8). While the fundamental biology of RSV remains conserved, multiple studies have reported that clinical outcomes may be influenced by specific, clade-defining mutations (9–16). However, this association is subject to debate owing to the influence of confounding factors such as patient age, prematurity, comorbidities, prior immunity, environmental factors, demographic and geographic variability, as well as heterogeneity in severity metrics and study methodologies (17–20).

Upon entering the human respiratory tract, RSV initiates a highly coordinated infection process driven by its eleven proteins encoded in a ~15,000 base pair negative-sense RNA genome. Collectively, the concerted actions of these eleven proteins – NS1, NS2, N, P, M, SH, G, F, M2-1, M2-2, and L – enable RSV to induce the profound airway inflammation and epithelial injury frequently associated with RSV disease. There is a critical knowledge gap in linking specific RSV genotypes to clinical severity through integrated genomic, structural, and functional analyses (9,19). A barrier to further reducing the burden of RSV disease is the incomplete understanding of the viral and host determinants that drive the heterogeneity of clinical outcomes. This proof-of-concept study investigated the hypothesis that specific amino acid polymorphisms in RSV are associated with clinical disease severity by means of comparative genomics. We sequenced RSV isolates from children enrolled at Connecticut Children's during a single

season and correlated differences in the viral protein sequences with validated clinical disease severity scores.

Methods

Subjects and biospecimens

We selected eligible subjects with RSV who had been enrolled as controls in a single-center COVID-19 biorepository from November 2022 to March 2023 (IRB approval #20-055). Inclusion criteria for the current study were defined as subjects under 24 months of age who were hospitalized for treatment of RSV mono-infection confirmed by a commercial RT-PCR assay. Demographic data were collected via in-person surveys and clinical data were abstracted from inpatient records. The primary outcome was defined by the previously validated Clinical Disease Severity Score (CDSS) based on the subject's most severe condition during their hospitalization (**S1 Table**) (22). The CDSS is an objective measure comprised of five parameters: 1) respiratory rate, 2) auscultation, 3) transcutaneous O_2 saturation, 4) retraction, and 5) activity level (mainly assessed by feeding difficulty). Each parameter ranks from 0 (normal) to 3 (most abnormal), and subjects were classified as having mild (0-5), moderate (6-10), or severe (11-15) RSV (22). Mid-turbinate nasal fluid was collected at time of enrollment using BD Universal Viral Transport Collection Kits (ThermoFisher Scientific, Cat #B220529). Vials were vortexed for 20 seconds, media was divided into 500 μL aliquots, and samples were stored at -80 °C until used.

Isolation of RNA from Mid-turbinate nasal swabs and total RNA QC

RNA was isolated from mid-turbinate nasal swab specimens using the Direct-zol™ RNA Miniprep Kit (Zymo Research) according to the manufacturer's instructions. Total RNA was quantified and purity ratios determined for each sample using the NanoDrop 2000 spectrophotometer (ThermoFisher Scientific, Waltham, MA, USA). To further assess RNA quality, total RNA was analyzed on the Agilent TapeStation 4200 (Agilent Technologies, Santa Clara, CA, USA) using the RNA High Sensitivity assay.

Illumina RNA Enrichment Library preparation and Sequencing

Total RNA samples were prepared for RNA enrichment using the Illumina RNA for Enrichment Sample Preparation with the Respiratory Virus Oligo Panel (RVOP) following the manufacturer's protocol (Illumina, San Diego, CA, USA). Libraries were validated for length and adapter dimer removal using the Agilent TapeStation 4200 D1000 High Sensitivity assay (Agilent Technologies, Santa Clara, CA, USA), then quantified and normalized using the dsDNA High Sensitivity Assay for Qubit 3.0 (Life Technologies, Carlsbad, CA, USA). Sample libraries were prepared for Illumina sequencing by denaturing and diluting the libraries per manufacturer's protocol (Illumina, San Diego, CA, USA). All samples were pooled into one sequencing pool, equally normalized, and run as one sample pool across the Illumina NovaSeq 6000 using version 1.5 chemistry. Target read depth of 2M reads was achieved per sample with paired end 100bp reads.

Sequence analysis pipeline

Viral genomic analysis was performed using Illumina paired-end sequencing data processed through a reference-guided assembly pipeline. Raw reads underwent quality control with FastP and FastQC software, which trimmed low-quality bases (Q-score <20) and adapter sequences. To exclude non-RSV genetic material, unassembled but trimmed reads were taxonomically classified with Kraken2 software (23) against the standard Kraken Database. Only sequences assigned to Human orthopneumovirus (RSV taxon ID: 208895) were filtered and retained using SeqTK software. Filtered RSV-specific reads were aligned to the RSV-A reference genome (NCBI accession: KT992094.1) using BWA-MEM (v0.7.17) [28] with default settings. Consensus RSV genomes generated through reference-guided assembly were annotated using VIGOR4 (24).

Sequence comparisons and analysis of point mutations

Genomes of the RSV clinical isolates were analyzed using Nextstrain's web-based platform, Nextclade (v3.13.2) (25) to assign clades, identify mutations, and perform additional quality checks. Sequences were

137 aligned with global RSV-A genomes from GenBank via Nextstrain's automated pipeline. For mutation
138 profiling, Nextstrain's variant-calling module identified amino acid polymorphisms relative to the RSV A
139 reference (EPI_ISL_412866). Clade classification followed Nextstrain's nomenclature, supported by
140 bootstrap values >70%.
141
142 *Culture of RSV from clinical isolates*
143 A549 cells (ATCC CC-185) were seeded in DMEM (Gibco, Ref # 31966-021) + 1% GlutaMAX (Gibco,
144 35050-061) supplemented with 10% fetal bovine serum (Gibco, Ref# A56707-01) and 1% Anti-Anti
145 (Gibco, Ref # 15240-062). Cells were allowed to adhere overnight. After 12 hours post-seed
146 (approximately 95% confluent cells) were infected with each clinical isolate at an MOI of 0.01 for 2
147 hours. Inoculum was removed, cells were washed with PBS (Gibco, Ref# 2085290), and cell culture
148 media was added. Plates were incubated in 5% CO_2 at 37 °C for 24, 48, 72, or 96 hours post-infection
149 (HPI).
150
151 *Determination of viral load*
152 Extracellular viral load was determined using the 50% tissue culture infectious dose ($TCID_{50}$) assay. The
153 $TCID_{50}$ assay was performed by infecting approximately 95% confluent A549 cell cultures cells in 96-
154 well plates. Serial tenfold dilutions of each sample were prepared in eight replicates in infection medium.
155 After washing the cell monolayers, 100 µL of each dilution was added per well and incubated at 37°C for
156 2 hours. An additional 75 µL of infection medium was then added, and plates were incubated for 4–5
157 days. After incubation, infection medium was aspirated then cells were fixed and stained with crystal
158 violet. $TCID_{50}$ was calculated using the Reed-Muench method.
159
160 *Structural Analyses*

161 L polymerase structure predictions were obtained using homology-based modelling based on RSV RNA
162 polymerase (PDB: 6UEN). N-linked and O-linked glycosylation predictions were performed using
163 NetNGlyc 1.0 (30) and NetOGlyc 4.0 (31), respectively.

164 **Results/Discussion**

165 This proof-of-concept study provides insights into molecular determinants of RSV virulence by
166 integrating genomic and phenotypic analyses with measures of clinical disease severity. After excluding
167 three subjects due to co-detection of SARS-CoV-2 (n=1), adenovirus (n=1), rhinovirus/enterovirus (n=1),
168 we analyzed RSV isolates from five infants who had no comorbidities (**Table 1**). Nasal samples from the
169 five subjects were collected a median of five days after start of symptoms (IQR, 4 - 6 days). Two subjects
170 were scored as having severe RSV disease (Isolate 090, Isolate 104), one scored as moderate RSV disease
171 (Is. 101), and two scored as mild RSV disease (Is. 081, Is. 084). One subject with severe disease was
172 admitted to the intensive care unit. All subjects received oxygen therapy via nasal cannula.
173
174 Genome sequencing and comparative analysis of the five RSV isolates revealed that all belonged to RSV-
175 A and the GA2.3.5 G clade. Isolates from mild cases clustered in the A.D clade with moderate and severe
176 cases clustering in the A.D.1.5 and A.D.1.8 subclades (**Figure 1**). Comparative analysis of amino acid
177 polymorphisms in RSV between mild and moderate/severe disease isolates revealed multiple non-
178 synonymous substitutions. Amino acid differences at 19 positions were identified that distinguished all
179 mild isolates from all moderate/severe isolates (**Table 2**). Of the 19 identified, the majority were found to
180 be in the G protein (n=8) and the L polymerase (n=5). Others were found in the F protein (n=1), M
181 protein (n=1), P protein (n=1), M2-1 protein (n=1), and M2-2 (n=2). Many are associated with altered
182 physicochemical properties as shown in **Table 2**, which may contribute to differences in RSV disease
183 severity observed in hospitalized children.
184

185 In vitro growth kinetics of all RSV isolates in A549 cells demonstrated that isolates from moderate/severe
186 cases replicated more rapidly than those from mild cases; isolates from moderate/severe cases showed
187 significantly greater mean levels of extracellular viral titers than those from mild cases at 72 and 96-hours
188 post-infection (two-way ANOVA with Tukey's multiple-comparison test, $p<0.05$) (**Figure 2**).
189 Importantly, the phenotypic differences in viral replication in the present study were observed in a
190 controlled cell culture system, which reflects intrinsic viral properties because the influence of host-
191 related confounding variables was removed.
192
193 Given the evidence that isolates from moderate/severe RSV disease replicate to higher titers than those
194 from mild cases (**Figure 2)**, we employed predictive protein modeling to elucidate the structural
195 consequences of associated mutations. Structural modeling suggested that these mutations, particularly in
196 the L and G proteins, may enhance viral fitness by altering protein stability, dimerization, and host
197 interaction. All isolates encoded a 321-aa G protein. N-glycosylation prediction showed a stepwise
198 increase with severity: mild isolates had two sites, moderate/severe had three to four (**S1 Figure**). A
199 previous report demonstrated that glycosylation of the C-terminal domain of the G protein reduced
200 reactivity with specific antibodies, suggesting that various glycosylation patterns of RSV may contribute
201 to evasion of the host's humoral immune response (26).
202
203 L polymerase sequences revealed five amino acid differences between mild and moderate/severe isolates:
204 two in the RdRp domain (143, 179) and three within the connector region (1653, 1661, 1715) (**Table 2**).
205 Structural modeling based on Protein Data Bank 6UEN (27) highlighted these substitutions but limited
206 interpretation to the experimentally resolved RdRp and capping regions (**S2 Figure**). An additional
207 aspartate residue in the finger domain of the RSV L protein, specifically at position AA143, may have
208 significant implications for polymerase function. Introduction of an additional aspartate in this region
209 could alter the electrostatics of the template entry pore or influence RNA binding affinity (28,29). Such

210 changes may impact processivity or regulation of RNA synthesis, thereby affecting viral replication
211 efficiency and, consequently, clinical outcomes.
212
213 Reported associations between RSV viral load and disease severity in young children have been
214 inconsistent, likely due to variations in study design, analytical methods, host immune responses, and
215 intrinsic viral factors. Although our sample size is small, the compelling molecular findings presented
216 here highlight the potential for specific pathoadaptive mutations to influence evolving RSV virulence and
217 clinical outcomes. These results may help to explain previously reported inconsistencies and highlight the
218 need for larger studies, reverse genetics, and in vivo models to elucidate the specific mechanisms by
219 which RSV phenotype shapes disease severity.
220
221 **Acknowledgments:** We would like to express our immense gratitude to our colleagues Carlie DeFelice,
222 Dr. Kelly Hawley, Judy Kalinowski, Carson Karanian, Stephanie Lesmes, Dr. Bo Reese, and Jordan Wolf
223 for their vital contribution to the project, including participant recruitment, biospecimen collection,
224 processing and testing, and data capture.
225 **References**

226 1. Mazur NI, Caballero MT, Nunes MC. Severe respiratory syncytial virus infection in children: burden,
227 management, and emerging therapies. The Lancet. 2024 Sept 21;404(10458):1143–56.

228 2. Jain S, Williams DJ, Arnold SR, Ampofo K, Bramley AM, Reed C, et al. Community-acquired
229 pneumonia requiring hospitalization among U.S. children. N Engl J Med. 2015 Feb 26;372(9):835–
230 45.

231 3. Li Y, Wang X, Blau DM, Caballero MT, Feikin DR, Gill CJ, et al. Global, regional, and national
232 disease burden estimates of acute lower respiratory infections due to respiratory syncytial virus in
233 children younger than 5 years in 2019: a systematic analysis. The Lancet. 2022 May
234 28;399(10340):2047–64.

235 4. Andeweg S, Schepp R, van de Kassteele J, Mollema L, Berbers G, van Boven M. Population-based
236 serology reveals risk factors for RSV infection in children younger than 5 years. Sci Rep.
237 2021;11(1):8953.

238 5. Abrams EM, Doyon-Plourde P, Davis P, Brousseau N, Irwin A, Siu W, et al. Burden of disease of
239 respiratory syncytial virus in infants, young children and pregnant women and people. Can Commun
240 Dis Rep. 50(1–2):1–15.

6. Halasa N, Zambrano L, Amarin J, Stewart L, Newhams M, Levy E, et al. Infants admitted to US intensive care units for RSV infection during the 2022 seasonal peak. JAMA Netw Open. 2023;6(8):e2328950.

7. Shishir TA, Saha O, Rajia S, Mondol SM, Masum MHU, Rahaman MM, et al. Genome-wide study of globally distributed respiratory syncytial virus (RSV) strains implicates diversification utilizing phylodynamics and mutational analysis. Sci Rep. 2023 Aug 19;13(1):13531.

8. Yu JM, Fu YH, Peng XL, Zheng YP, He JS. Genetic diversity and molecular evolution of human respiratory syncytial virus A and B. Sci Rep. 2021 June 21;11(1):12941.

9. Bender W, Zhang Y, Corbett A, Chu C, Grier A, Wang L, et al. Association of disease severity and genetic variation during primary Respiratory Syncytial Virus infections. BMC Medical Genomics. 2024 June 19;17(1):165.

10. Fletcher J, Smyth R, Thomas H, Ashby D, Hart C. Respiratory syncytial virus genotypes and disease severity among children in hospital. Arch Dis Child. 1997 Dec;77(6):508–11.

11. Human S, Hotard A, Rostad C, Lee S, McCormick L, Larkin E, et al. A respiratory syncytial virus attachment gene variant associated with more severe disease in infants decreases fusion protein expression, which may facilitate immune evasion. J Virol. 2020;95(2).

12. Li W, Wang Y, Yu B, Tan Q, Zhou J, Hu J, et al. Disease severity of respiratory syncytial virus (RSV) infection correlate to a novel set of five amino acid substitutions in the RSV attachment glycoprotein (G) in China. Virus Research. 2020 May 1;281:197937.

13. Midulla F, Nenna R, Scagnolari C, Petrarca L, Frassanito A, Viscido A, et al. How Respiratory Syncytial Virus Genotypes Influence the Clinical Course in Infants Hospitalized for Bronchiolitis. The Journal of Infectious Diseases. 2019 Jan 29;219(4):526–34.

14. Comas-García A, Noyola DE, Cadena-Mota S, Rico-Hernández M, Bernal-Silva S. Respiratory Syncytial Virus-A ON1 Genotype Emergence in Central Mexico in 2009 and Evidence of Multiple Duplication Events. J Infect Dis. 2018 Mar 13;217(7):1089–98.

15. Esposito S, Piralla A, Zampiero A, Bianchini S, Di Pietro G, Scala A, et al. Characteristics and Their Clinical Relevance of Respiratory Syncytial Virus Types and Genotypes Circulating in Northern Italy in Five Consecutive Winter Seasons. PLoS One. 2015;10(6):e0129369.

16. Oraby AK, Stojic A, Elawar F, Bilawchuk LM, McClelland RD, Erwin K, et al. A single amino acid mutation alters multiple neutralization epitopes in the respiratory syncytial virus fusion glycoprotein. npj Viruses. 2025 Apr 22;3(1):1–14.

17. Bøås H, Havdal LB, Størdal K, Døllner H, Leegaard TM, Bekkevold T, et al. No association between disease severity and respiratory syncytial virus subtypes RSV-A and RSV-B in hospitalized young children in Norway. PLoS One. 2024;19(3):e0298104.

18. Lin GL, Drysdale SB, Snape MD, O'Connor D, Brown A, MacIntyre-Cockett G, et al. Targeted metagenomics reveals association between severity and pathogen co-detection in infants with respiratory syncytial virus. Nat Commun. 2024 Mar 16;15(1):2379.

19. Anderson LJ, Peret TC, Piedra PA. RSV Strains and Disease Severity. The Journal of Infectious Diseases. 2019 Jan 29;219(4):514–6.

20. Vandini S, Biagi C, Lanari M. Respiratory syncytial virus: The influence of serotype and genotype variability on clinical course of infection. Int J Mol Sci. 2017;18(8).

21. CDC. RESP-NET. 2025 [cited 2025 Nov 18]. Respiratory Virus Hospitalization Surveillance Network (RESP-NET). Available from: https://www.cdc.gov/resp-net/dashboard/index.html

22. Mejias A, Dimo B, Suarez NM, Garcia C, Suarez-Arrabal MC, Jartti T, et al. Whole blood gene expression profiles to assess pathogenesis and disease severity in infants with respiratory syncytial virus infection. PLoS Med. 2013 Nov;10(11):e1001549.

23. Wood DE, Lu J, Langmead B. Improved metagenomic analysis with Kraken 2. Genome Biology. 2019 Nov 28;20(1):257.

24. Wang S, Sundaram JP, Stockwell TB. VIGOR extended to annotate genomes for additional 12 different viruses. Nucleic Acids Res. 2012 July;40(Web Server issue):W186–92.

25. Aksamentov I, Roemer C, Hodcroft EB, Neher RA. Nextclade: clade assignment, mutation calling and quality control for viral genomes. Journal of Open Source Software. 2021 Nov 30;6(67):3773.

26. Rawling J, Melero JA. The Use of Monoclonal Antibodies and Lectins to Identify Changes in Viral Glycoproteins That are Influenced by Glycosylation. In: Sugrue RJ, editor. Glycovirology Protocols [Internet]. Totowa, NJ: Humana Press; 2007 [cited 2025 Nov 18]. p. 109–25. Available from: https://doi.org/10.1007/978-1-59745-393-6_8

27. Bank RPD. RCSB PDB - 6UEN: Cryo-EM structure of the respiratory syncytial virus RNA polymerase [Internet]. [cited 2025 Nov 18]. Available from: https://www.rcsb.org/structure/6UEN

28. Sutto-Ortiz P, Eléouët JF, Ferron F, Decroly E. Biochemistry of the Respiratory Syncytial Virus L Protein Embedding RNA Polymerase and Capping Activities. Viruses. 2023 Jan 25;15(2):341.

29. Liang B. Structures of the Mononegavirales Polymerases. J Virol. 2020 Oct 27;94(22):e00175-20.

30. Gupta R, Brunak S. Prediction of glycosylation across the human proteome and the correlation to protein function. Pac Symp Biocomput. 2002;310–22.

31. Steentoft C, Vakhrushev SY, Joshi HJ, Kong Y, Vester-Christensen MB, Schjoldager KTBG, et al. Precision mapping of the human O-GalNAc glycoproteome through SimpleCell technology. EMBO J. 2013 May 15;32(10):1478–88.

Table 1. Cohort Characteristics

Characteristic	RSV Cohort (n=5)
Enrollment Age (mos)	9 (3-9)
Male	4 (80%)
Race	
White	2 (40%)
Black	1 (20%)
Other	2 (40%)
Hispanic	3 (60%)
Length of Stay (days)	2 (1-3)
CDSS Category	
Mild	2 (40%)
Moderate	1 (20%)
Severe	2 (40%)

Data given as median (IQR) or n (%)

Table 2. Amino Acid Differences and side chain characteristics distinguishing Mild from Moderate/Severe

Protein	AA #	Mild (Is. 081, Is. 084)		Moderate/severe (Is. 090, Is. 101, Is. 104)	
L	143	N	HYDROPHILIC	D	NEGATIVE
L	179	T	HYDROPHILIC	S	HYDROPHILIC
L	1653	I	HYDROPHILIC	V	HYDROPHILIC
L	1661	K	POSITIVE	N	HYDROPHILIC
L	1715	S	HYDROPHILIC	N	HYDROPHILIC
G	105	T	HYDROPHILIC	S	HYDROPHILIC
G	123	K	POSITIVE	E	NEGATIVE
G	142	L	HYDROPHOBIC	S	HYDROPHILIC
G	281	K	POSITIVE	T	HYDROPHILIC
G	283	F	AROMATIC	S	HYDROPHILIC
G	294	S	HYDROPHILIC	P	PROLINE
G	309	H	POSITIVE	Y	HYDROPHOBIC
G	310	P	PROLINE	L	HYDROPHOBIC
M2-1	172	A	HYDROPHOBIC	T	HYDROPHILIC
M2-2	9	E	NEGATIVE	D	NEGATIVE
M2-2	49	T	HYDROPHILIC	P	PROLINE
F	555	A	HYDROPHOBIC	T	HYDROPHILIC
M	43	M	HYDROPHOBIC	I	HYDROPHOBIC
P	62	T	HYDROPHILIC	I	HYDROPHOBIC

A

Study ID Number	CDSS	Clade	G Clade	Genome Coverage
Isolate 081	mild (0-5)	A.D	GA2.3.5	100%
Isolate 084	mild (0-5)	A.D	GA2.3.5	100%
Isolate 090	severe (10-15)	A.D.1.8	GA2.3.5	100%
Isolate 101	moderate (6-9)	A.D.1.8	GA2.3.5	100%
Isolate 104	severe (10-15)	A.D.1.5	GA2.3.5	100%

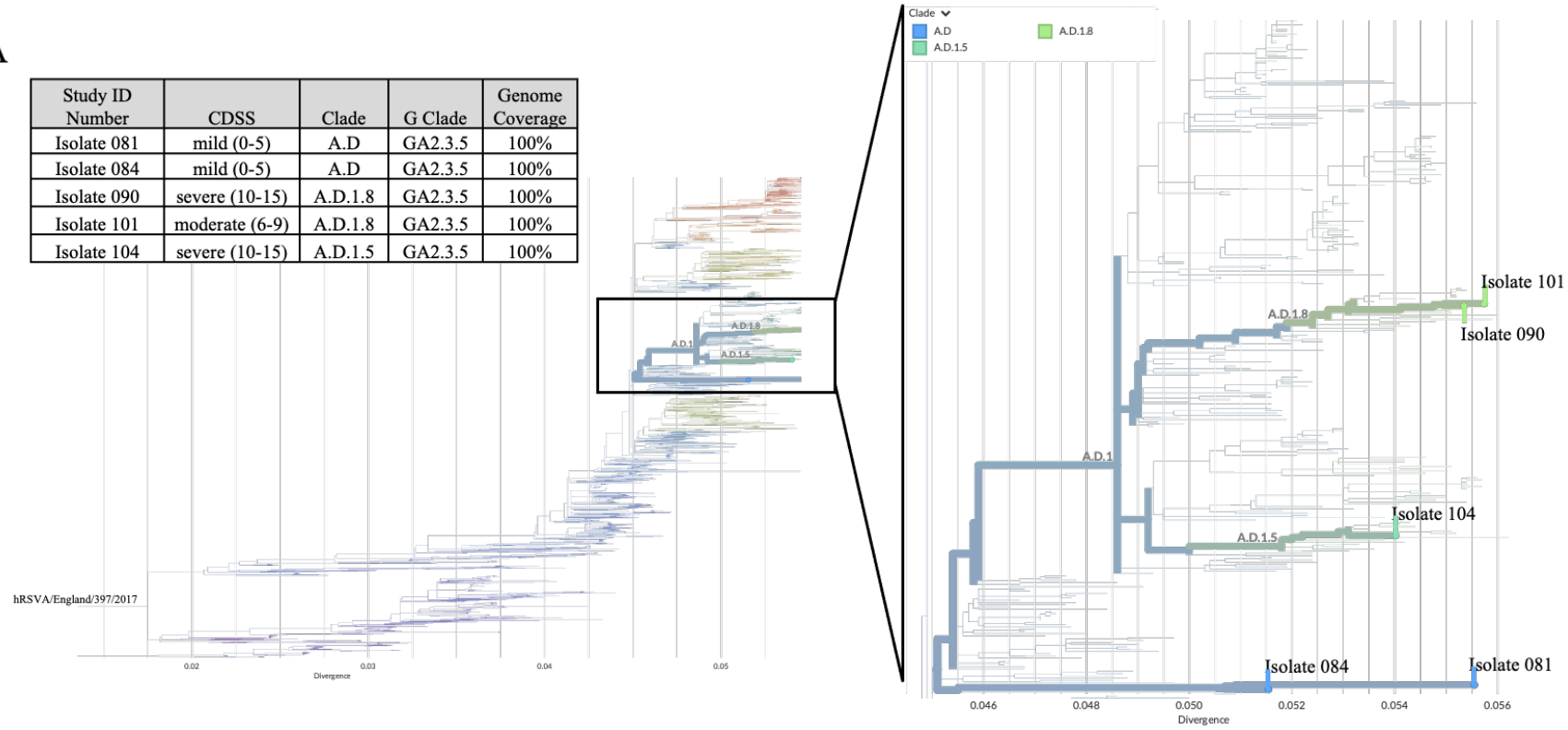

Figure 1. Phylogenetic analysis of RSV clinical isolates. CDSS, Clinical Disease Severity Score

A

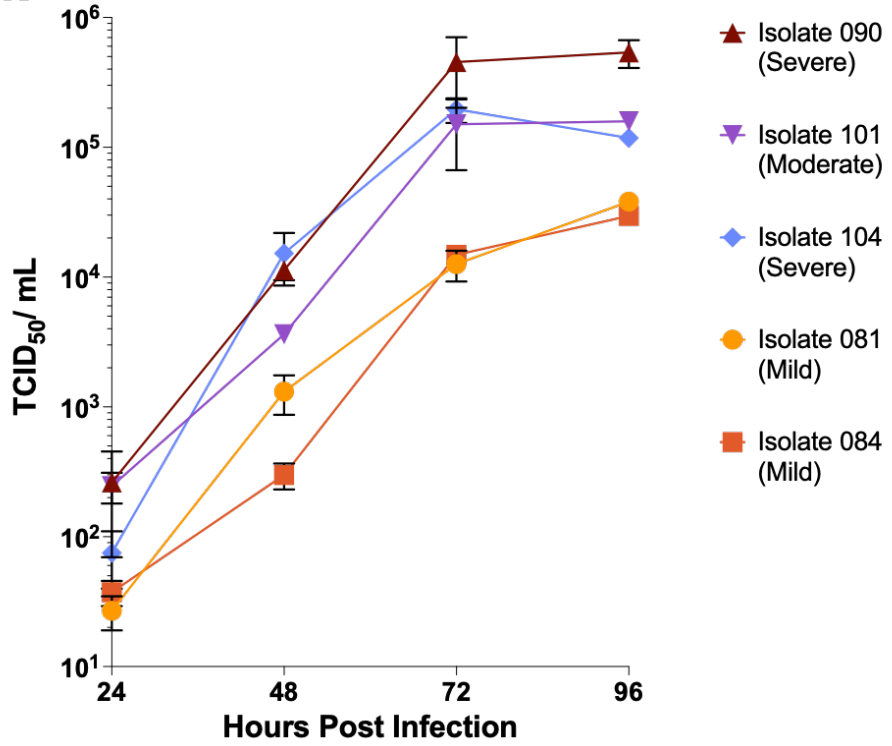

B

		24 HPI		
		Is. 090 (Severe)	Is. 101 (Moderate)	Is. 104 (Severe)
24 HPI	Is. 081 (Mild)	ns	ns	ns
	Is. 084 (Mild)	ns	ns	ns

		48 HPI		
		Is. 090 (Severe)	Is. 101 (Moderate)	Is. 104 (Severe)
48 HPI	Is. 081 (Mild)	ns	ns	ns
	Is. 084 (Mild)	ns	ns	ns

		72 HPI		
		Is. 090 (Severe)	Is. 101 (Moderate)	Is. 104 (Severe)
72 HPI	Is. 081 (Mild)	*	**	**
	Is. 084 (Mild)	*	*	*

		96 HPI		
		Is. 090 (Severe)	Is. 101 (Moderate)	Is. 104 (Severe)
96 HPI	Is. 081 (Mild)	*	ns	ns
	Is. 084 (Mild)	****	ns	ns

Figure 2. Temporal analysis of RSV isolate replication **A)** A549 cells were infected with RSV isolates at an MOI of 0.01. Extracellular RSV was isolated, and viral titer was determined by $TCID_{50.}$ Samples were collected at 24H intervals over 96 hours. Data shown represent the mean of duplicate measurements +/- SD **B)** Table summarizing the statistical significance of differences in viral titer between mild, moderate, and severe strains at each timepoint. ns (not significant), * ($p < 0.05$), ** ($p < 0.01$), *** ($p < 0.001$), **** ($p < 0.0001$). Abbreviations: $TCID_{50}$, 50% tissue culture infectious dose; MOI, multiplicity of infection; Is, Isolate; HPI, Hours post-infection.

Supplemental Information

S1 Table. Clinical Disease Severity Score (CDSS)

	0	**1**	**2**	**3**
O_2 Saturation	>95% in RA	92%-95% in RA	<92% in RA or suppl O_2 ≤35%	Intubated/CPAP or suppl O2>35%
Respiratory Rate	≤6 m <40/min >6 m <30/min	≤6 m 41-55/min >6 m 31-45/min	≤6 m 56-70 >6 m 46-60	≤6 m >70 >6 m >60
Retractions	No	Subcostal +	Subcostal ++ or intercostal	Subcostal +++ or intercostal and suprasternal
Auscultation	Normal	Crackles/ ronchi	Any wheezing	Exp/insp wheezing without stethoscope or no breath sounds heard
Activity	Normal, alert	Abnormal, fussy, or decreased oral intake	Unable to maintain hydration (IV fluids or NG feeds)	Intubated

[a]Score from 0-15: Mild (0-5), Moderate (6-9), Severe (≥10).
[b]CPAP, continuous positive airway pressure; exp, expiratory; insp, inspiratory; IV, intravenous; m, months; min, minute; NG, nasogastric tube; O_2, oxygen; RA, room air; suppl, supplemental; +, mild; ++, moderate; +++, severe.

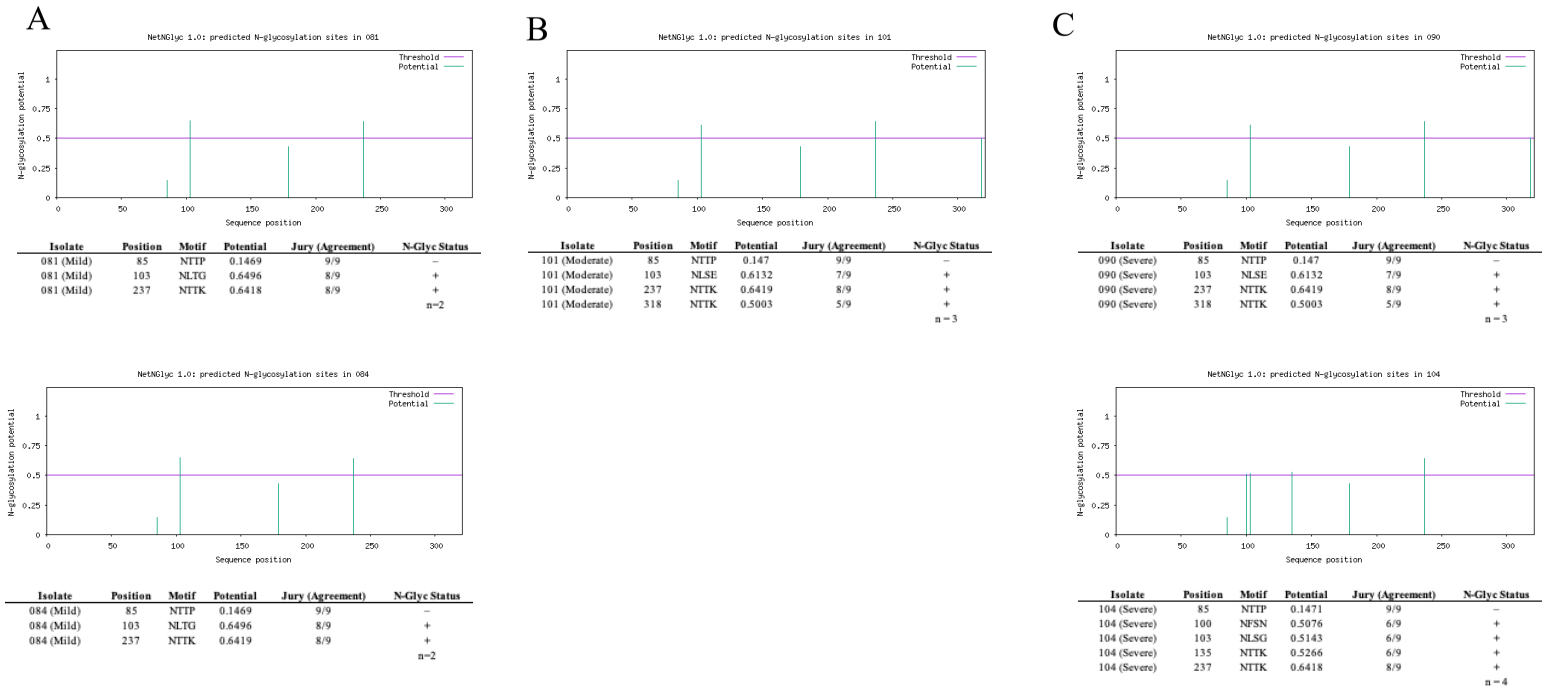

Isolate	Position	Motif	Potential	Jury (Agreement)	N-Glyc Status
081 (Mild)	85	NTTP	0.1469	9/9	–
081 (Mild)	103	NLTG	0.6496	8/9	+
081 (Mild)	237	NTTK	0.6418	8/9	+
					n=2

Isolate	Position	Motif	Potential	Jury (Agreement)	N-Glyc Status
101 (Moderate)	85	NTTP	0.147	9/9	–
101 (Moderate)	103	NLSE	0.6132	7/9	+
101 (Moderate)	237	NTTK	0.6419	8/9	+
101 (Moderate)	318	NTTK	0.5003	5/9	+
					n = 3

Isolate	Position	Motif	Potential	Jury (Agreement)	N-Glyc Status
090 (Severe)	85	NTTP	0.147	9/9	–
090 (Severe)	103	NLSE	0.6132	7/9	+
090 (Severe)	237	NTTK	0.6419	8/9	+
090 (Severe)	318	NTTK	0.5003	5/9	+
					n = 3

Isolate	Position	Motif	Potential	Jury (Agreement)	N-Glyc Status
084 (Mild)	85	NTTP	0.1469	9/9	–
084 (Mild)	103	NLTG	0.6496	8/9	+
084 (Mild)	237	NTTK	0.6419	8/9	+
					n=2

Isolate	Position	Motif	Potential	Jury (Agreement)	N-Glyc Status
104 (Severe)	85	NTTP	0.1471	9/9	–
104 (Severe)	100	NFSN	0.5076	6/9	+
104 (Severe)	103	NLSG	0.5143	6/9	+
104 (Severe)	135	NTTK	0.5266	6/9	+
104 (Severe)	237	NTTK	0.6418	8/9	+
					n = 4

S1 Figure. Predicted N-glycosylation sites in RSV Attachment G protein A) in isolates from cases of mild disease (Is. 081, Is. 084), B) in isolates from moderate cases of disease (Is. 101) and C) in isolates from severe cases of disease (Is. 090, Is. 104). N-glycosylation potential threshold = 0.5 (purple line). Potential is the predicted likelihood of glycosylation (green). Jury is the number of prediction tools in agreement out of 9.

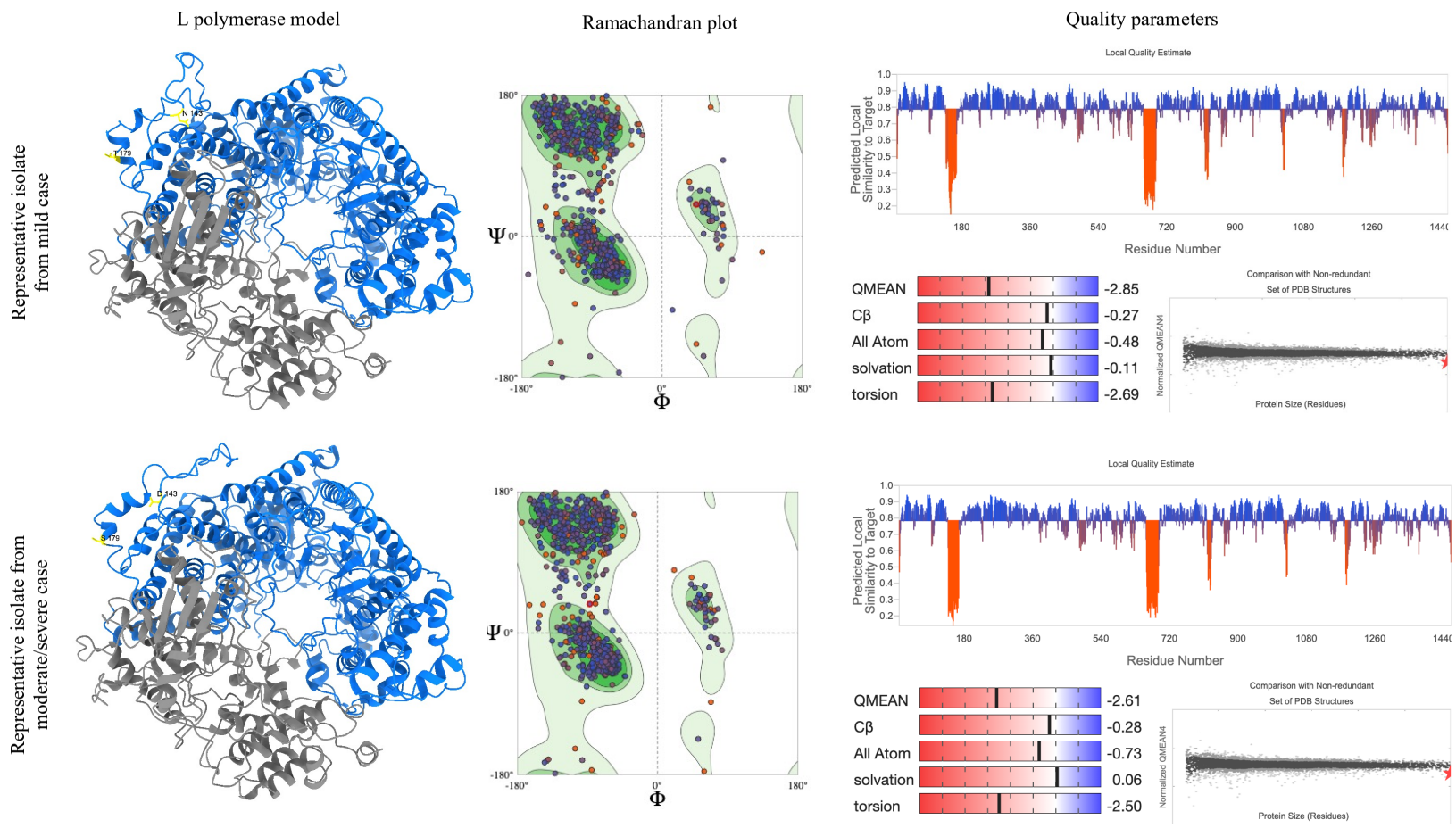

S2 Figure. Structural model of RSV L proteins of representative isolates from mild and moderate/severe cases using homology modelling based on the RSV polymerase complex structure (PDB: 6UEN). Ribbon representation of L proteins are shown on left (yellow, pathoadaptive mutations; blue, RNA-dependent RNA polymerase domain; grey, PRNTase capping domain). Ramachandran plots are shown for each model (center) followed by quality parameters of each model. T, Threonine; N, Asparagine; S, Serine; D, Aspartate;